PAPER

NJC
www.rsc.org/njc

How humidity affects the solid-state inclusion of 2-phenoxyethanol in β-cyclodextrin: a comparison with β-cyclodextrin

Luís Cunha-Silva and José J. C. Teixeira-Dias*

Department of Chemistry, CICECO, University of Aveiro, P-3810-193, Aveiro, Portugal. E-mail: tdias@dq.ua.pt; Fax: 351 234370084; Tel: 351 234370360

Received* (in London, UK) *7th August 2003, Accepted 27th October 2003
First published as an Advance Article on the web 1st December 2003

The solid-state inclusion compound ({βCD·PhE}) of 2-phenoxyethanol (PhE) in β-cyclodextrin (βCD) was prepared from aqueous solution and studied by powder X-ray diffraction (PXRD), thermogravimetric analysis (TGA), FT-Raman and ^{13}C CP MAS NMR, at ambient humidity and several defined relative humidites (RHs). It is shown that {βCD·PhE} is a true inclusion microcrystalline compound whose PXRD pattern best matches that of an isostructural channel compound. The studies at defined RHs show that its crystalline structure is preserved for RHs equal or above 20% and that its hydration water is not as strongly bound as in βCD. Relative intensities of βCD Raman bands generally ascribed to C–O stretching and CH_2 bending vibrations are found to be influenced by the presence of the guest in the βCD cavity or the increase of ambient humidity, or by both of these factors. Comparison of the ^{13}C CP MAS NMR spectra for {βCD·PhE} with those for βCD, at RHs equal or higher than 20%, reveals a decrease in the multiplicities of the carbon atoms resonances and in the dispersions of chemical shift values of the various types of carbon atoms, thus pointing to an improved symmetrization of the βCD macrocycle in the channel structure of {βCD·PhE}.

Introduction

Crystalline hydrates of β-cyclodextrin (cyclomaltoheptaose, βCD, Scheme 1) are good models for the study of hydration processes in biomolecular systems, exhibiting interesting properties which have been the subject of a number of studies.[1–8] First of all, the herring bone crystal structure—a cage type structure—is known to be preserved for humidities greater than 15%, though with a 2.3% reduction of the cell volume with respect to the 100% humidity level.[1] In the range of humidities from 15 to 100%, the water content of the crystalline βCD hydrate is in fast equilibrium with atmospheric humidities and, despite the fact that the crystal lattice does not have permanent channels, fast diffusion of water molecules, estimated at 1/30 of the bulk water value, is known to occur due to transient fluctuations in the lattice.[1] Exchange experiments carried out with water marked either with D or ^{18}O showed that the H/D exchange was found to be complete, hence extending also to sterically unaccessible O–H groups, and that the long-range transport of hydrogen takes place by diffusion of intact water molecules.[2] In addition, βCD hydrates have also been investigated by ^{13}C CP MAS NMR as a part of a study for discovering the relationship between the glycosidic linkage conformations and the solid-state ^{13}C chemical shifts.[9–11] The wide range of chemical shifts observed for C1 and C4 sites were found to be primarily determined by the orientations of the glucose units in the βCD macrocycle and correlations were found between C1 chemical shifts and the moduli of torsion angles describing rotation about the C1–O1 and O1–C4′ bonds.[9] In turn, the chemical shifts for C6 resonances were found to be sensitive to hydrogen bonding interactions.[12] On the whole, the carbon atoms of the βCD macrocycle are interesting NMR probes for assessing conformational changes during hydration or dehydration processes.

While many studies based on the evaluation of physical and chemical properties of crystalline βCD hydrates have been performed during the last number of years, consideration of the hydration properties of βCD inclusion compounds have not recieved the same attention. In this work, the solid-state βCD inclusion compound of 2-phenoxyethanol (Scheme 1) was obtained by precipitation from aqueous solution, and its properties at various relative humidities (RHs) were studied by powder X-ray diffraction (PXRD), thermogravimetry, FT-Raman and ^{13}C CP MAS NMR. While it is generally accepted that hydration water is known to have an important role in promoting the stability of the inclusion compound, no systematic study of the hydration features of the compound resulting from the βCD inclusion of 2-phenoxyethanol has, to our knowledge, been done.

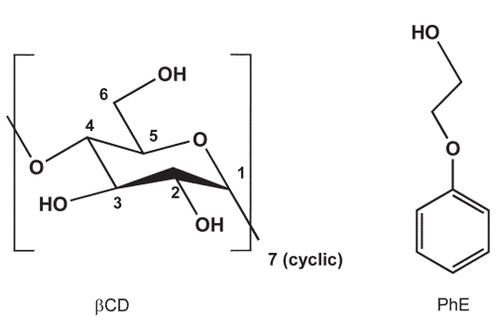

Scheme 1 Schematic representation of the βCD and PhE structures.

Experimental

General

βCD, kindly donated by Wacker-Chemie (München, Germany), was recrystallized from concentrated aqueous solution before use. 2-Phenoxyethanol (ethylene glycol phenyl ether), hereafter referred to as PhE (Ph stands for the phenoxy fragment and E for the $–CH_2CH_2OH$ moiety, respectively), was purchased from Aldrich and used as received. Lithium chloride hydrate (Riedel-de Haën), potassium acetate (Riedel-de Haën),

DOI: 10.1039/b309491j

zinc nitrate hexahydrate (Fluka), sodium bromide (Aldrich), sodium thiosulfate (Pronalab), ammonium chloride (Panreac) and ammonium dihydrogen phosphate (Panreac) were used for preparation of saturated salt solutions as received.

TGA studies were performed on a Mettler TA3000 system, using a heating rate of 1 °C min^{-1}, under nitrogen atmosphere, with a flow rate of 30 mL min^{-1}. The sample holder was a 5 mm Ø platinum plate and the sample mass was about 5–10 mg. Powder XRD data were collected on a Philips X'pert diffractometer using Cu-Kα radiation filtered by Ni (λ = 1.5418 Å). FT-Raman spectral studies (range 4000–100 cm^{-1}) were carried out on a Bruker RFS 100/S spectrometer, using a Nd/YAG laser line at 1064 μm, with 200–500 mW power (resolution 2–4 cm^{-1}, 100–2000 scans per spectrum). FTIR spectra (4000–400 cm^{-1}) were obtained on a Unican Mattson Model 7000 FTIR spectrometer, using KBr pellets (2 cm^{-1} resolution, 32 scans). Room-temperature solid-state ^{13}C CP MAS NMR spectra were recorded at 100.62 MHz, on a 9.4 T Bruker Avance 400 spectrometer (25 °C; 3.6 μs ^{1}H 90° pulses, 2.0 ms contact time, 7–8 kHz spinning rate; 4 s recycle delays). ^{1}H NMR spectrum of the inclusion compound was recorded at 300 MHz on a Bruker 300 Avance spectrometer, at 20 °C, on D_2O solution. Chemical shifts are quoted in parts per million (ppm) from TMS.

Preparation of the inclusion compound

The solid-state inclusion compound of PhE in βCD was prepared by a precipitation process. A saturated aqueous solution (2.8 mL H_2O) of βCD (0.491 g, 0.373 mmol) at 70 °C was heated to 80 °C and continuously stirred until complete dissolution of the solid. PhE (53.1 μL, 0.395 mmol) was added in a stoichiometric proportion and the resulting mixture was stirred at *ca.* 80 °C under reflux, during 24 h. The reaction mixture was then slowly cooled to room temperature and the obtained white precipitate was then filtered off, washed with cold distilled water, and exposed at room atmosphere for several days. Elemental analysis: calc. (%) for $C_{42}H_{70}O_{35}{\cdot}C_8H_{10}O_2{\cdot}10H_2O$: C 41.32, H 6.94, O 51.74; found C 40.96, H 7.22, O 51.82. ^{1}H NMR (300 MHz, D_2O, 20 °C, TMS): δ 7.29–7.24 (t, PhE), 6.97–6.91 (t, PhE), 4.95–4.94 (d, βCD), 4.05–4.02 (t, PhE), 3.86–3.79 (m, PhE and βCD), 3.74–3.69 (m, PhE and βCD), 3.54–3.50 (q, βCD), 3.49–3.43 (t, βCD). FTIR (KBr, cm^{-1}): 3357 (vs), 2923.6 (m), 1641(w), 1602 (w), 1588 (w), 1498 (w), 1455 (sh, w), 1433 (sh, w), 1413 (m), 1382 (sh, m), 1370 (m), 1335 (m), 1303 (m), 1248 (m), 1203 (w), 1158 (s), 1101 (s), 1080 (vs), 1056 (vs), 1030 (s), 1004 (s), 947 (m), 938 (m), 862 (w), 754 (m), 705 (m), 688 (m), 608 (m), 577 (m), 530 (m), 476 (w), 447 (w), 413 (w). ^{13}C CP MAS NMR: δ 158.3 (PhE, Ph), 128.8 (PhE, Ph), 120.4 (PhE, Ph), 114.9 (PhE, Ph), 103.8, 103.0 (βCD, C1), 83.2, 82.5, 81.5, 80.9, 80.4, 80.0 (βCD, C4), 73.8, 73.3, 72.5 (βCD, C2,3,5), 68.9 (PhE, CH_2), 62.0, 60.9, 60.6 (βCD, C6).

For simplicity, we will hereafter refer to the inclusion compound of PhE in βCD by the shorthand notation {βCD·PhE}. This nomenclature does not intend to make any reference to the stoichiometric ratio, since this was not determined in this paper for the solid-state inclusion compound. Incidentally, the stoichiometry of the inclusion complex in aqueous solution was determined by the continuous variation method (Job's method) and found to be 1:1.[13,14] This method involves running a series of experiments in which the ratio of host to guest initial concentrations is varied at well defined r values ($r = [\beta CD]_0/\{[\beta CD]_0 + [G]_0\}$), while maintaining constant the sum of the initial molar concentrations of host and guest ($[\beta CD]_0 + [G]_0$).

The 1:1 physical mixture was prepared by grinding an equimolar mixture of βCD (solid) and PhE (liquid) in a mortar.

Samples at defined RHs

In order to expose βCD and {βCD·PhE} to defined RHs, samples were stored during several days (one week at least) in contact with air of defined RHs set up by silica gel for RH = 0%, by various saturated salt solutions (RH = 15%, $LiCl{\cdot}H_2O$; RH = 20%, KCH_3COO; RH = 42%, $Zn(NO_3)_2{\cdot}6H_2O$; RH = 58%, $NaBr{\cdot}2H_2O$; RH = 78%, $Na_2S_2O_3{\cdot}5H_2O$; RH = 80%, NH_4Cl; RH = 93%, $NH_4H_2PO_4$),[1] and by pure water for RH = 100%.

Results and discussion

Powder X-ray diffraction (PXRD)

PXRD patterns for {βCD·PhE}, a reference isostructural inclusion compound {βCD·dodecenol} (powder diffractogram simulated from unit cell parameters, using the program Powdercell),[15,16] and βCD are shown in Fig. 1. As for the inclusion of PhE in βCD {βCD·PhE}, where this notation does not intend to specify a stoichiometry (presumably 1:1; see "Preparation of inclusion compound" in the Experimental Section), the notation "{βCD·dodecenol}" is used hereafter to simply represent the inclusion compound of dodecenol in βCD. In this case, each dodecenol molecule is included in a βCD dimer, thus originating a 2:1 stoichiometric ratio for the inclusion compound.[15]

The number of intense low angle reflections observed for {βCD·PhE} indicates that this inclusion compound precipitates as a microcrystalline powder. In addition, since its diffraction pattern does not match that for βCD, a different crystalline structure should have been formed, suggesting that a true inclusion solid-state compound was prepared.

PXRD can sometimes be used to quickly identify the type of crystal packing of cyclodextrin inclusion compounds using the concept of crystal isostructurality.[17,18] This concept applies to two or more crystalline phases that display identical or quasi-identical packing motifs. A prerequisite for isostructurality of two phases is the similarity of unit cell dimensions and of the internal arrangement of molecules. Within an isostructural series of crystalline inclusion compounds based on a particular cyclodextrin, the main features of the PXRD patterns should essentially coincide, regardless of the nature of the included guest.[17]

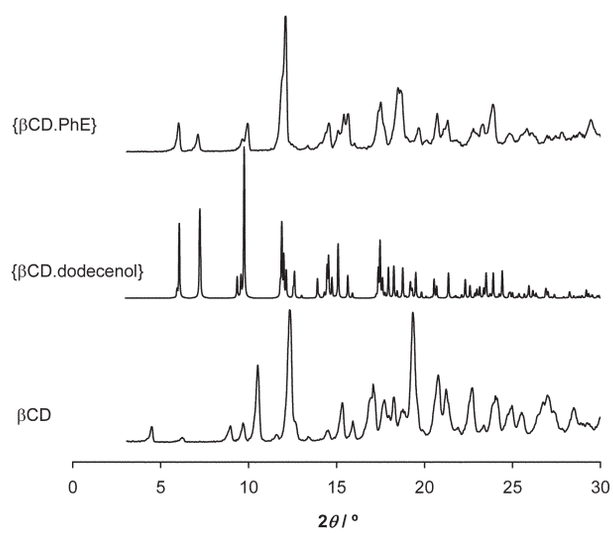

Fig. 1 PXRD patterns for {βCD·PhE}, {βCD·dodecenol} as a reference inclusion compound, and βCD. Samples of {βCD·PhE} and βCD were obtained at ambient humidity. The powder diffractogram for {βCD·dodecenol} was simulated from unit cell parameters using the program Powdercell.[15,16]

During the formation of inclusion compounds, βCD has a tendency to form head-to-head dimers held by multiple intermolecular O–H···O hydrogen bonds across the βCD secondary rims. These βCD dimers appear in inclusion compounds in a variety of 3D structural arrangements, classified as "channel", "intermediate", "chessboard" or "screw-channel".[17,18] Application of crystal isostructurality to {βCD·dodecenol} has allowed to ascribe this inclusion compound to a channel structure.[17] Using the program Powdercell,[16] a simulation of the PXRD pattern from the corresponding unit cell parameters yields 2θ values for the most intense peaks at about 6.1, 7.2, 9.7, 11.9, 14.5, 15.1, 17.4 and 18.7°. In turn, the {βCD·PhE} diffraction pattern, characterised by low angle peaks at 2θ values about 6.0, 7.0, 9.8, 12.0, 14.6, 15.4, 17.4 and 18.5°, matches well the {βCD·dodecenol} simulated PXRD pattern especially at low angles (2θ 3–20°), thus enabling us to suggest, for {βCD·PhE}, the same channel structure of {βCD·dodecenol}.

Fig. 2 presents a set of PXRD patterns for {βCD·PhE} at room temperature and defined RHs (0, 15, 20, 58 and 100%). For RHs between 20 and 58%, the PXRD patterns present reflections at the same angles, with gradable intensity variations. In turn, at RH 100%, two additional reflections appear at 2θ values 5.6 and 11.1°. Abrupt changes are also observed for RHs below 20%, *i.e.*, for RHs 15 and 0%. Lacking many of the reflections observed for higher RH values, these PXRD patterns only show two sharp and intense peaks at low angles, apart from a number of uncharacteristic weak and wide features, especially for $2\theta \geq 13°$. These observations suggest an appreciable loss of crystallinity at low water contents (RHs 15 and 0%), in particular, at RH 0%, thus pointing to the structural relevance of hydration water for preservation of the crystalline structure of {βCD·PhE}.

Fig. 3 shows the PXRD patterns for βCD at room temperature and defined RHs (0, 15, 20, 58 and 100%). While considerable differences are observed for the diffractogram at RH 0%, the other diffractograms present only gradual and minor alterations. In particular, only relative intensity changes are observed for RH above 15%, thus suggesting that the crystalline structure of βCD is essentially preserved for these RHs. In turn, a collapse of the crystalline structure is observed when passing from RH 15% to RH 0%, as previously mentioned.[1]

On the whole, the distinct crystal structures of {βCD·PhE} and βCD are both preserved for humidities ≥20% and 15%, respectively. Below these RH values, the crystalline structures collapse due to the loss of water. This observation points to the relevance of hydration water for the preservation of both crystalline structures and sets lower RHs for them to prevent collapse.

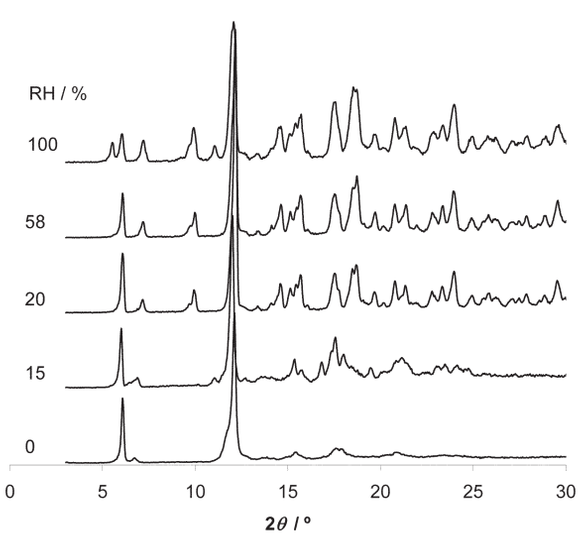

Fig. 2 PXRD patterns for samples of {βCD·PhE} prepared at defined RHs (0, 15, 20, 58, 100%).

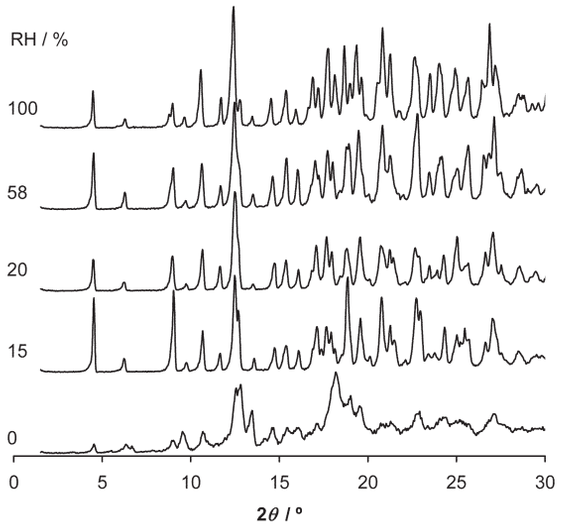

Fig. 3 PXRD patterns for samples of βCD prepared at defined RHs (0, 15, 20, 58, 100%).

Thermogravimetric analysis (TGA)

Fig. 4 shows the thermograms for {βCD·PhE}, the 1:1 physical mixture and βCD. Starting with βCD, one observes an initial loss of hydration water up to 80 °C (13.7% mass loss, corresponding to *ca.* 10 hydration water molecules per βCD molecule), with a single inflection point at 76 °C. No further mass change occurs until *ca.* 225 °C when melted βCD starts to decompose as shown by the abrupt mass loss whose differential thermogravimetric peak occurs at 285 °C.

The thermogram of the physical mixture can be interpreted in terms of the thermograms for the individual components. In it, steps can be seen corresponding, in sequence, to the dehydration of βCD, the release (vaporization) of PhE, and the decomposition of βCD.

In turn, the thermogram of {βCD·PhE} is qualitatively different from that of both the 1:1 physical mixture and βCD. After an initial mass loss of 6.6% up to 50 °C (inflection point occurs at 42 °C), ascribed to the loss of hydration water (approximately 5 hydration water molecules per βCD

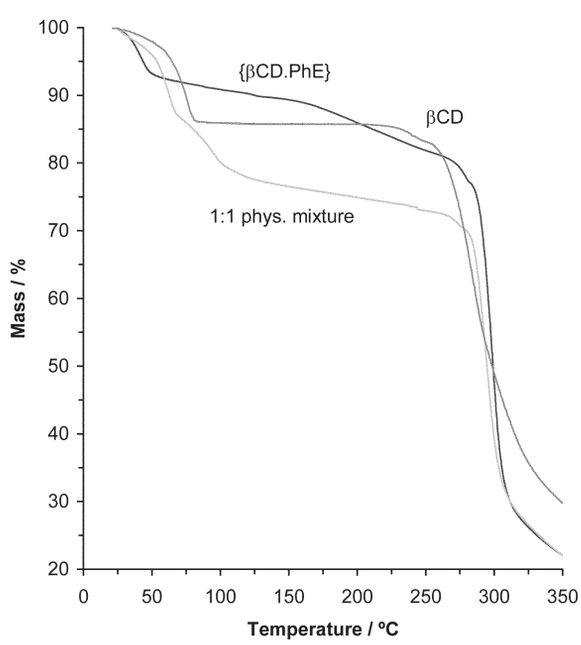

Fig. 4 Thermograms for samples of {βCD·PhE}, the 1:1 physical mixture of βCD and PhE, and βCD, prepared at ambient humidity.

molecule), two additional mass losses of 4.5% (segment line with small slope, from 50 to 168 °C) and 8.1% (segment line with a slightly higher slope, from 160 to 269 °C) should most likely correspond to the slow release (vaporization) of PhE following the dissociation of {βCD·PhE}. The step ascribed to the loss of hydration water in the {βCD·PhE} thermogram occurs before, *i.e.*, at lower temperature than the corresponding steps in the physical mixture and in βCD, and corresponds to a smaller mass loss, thus suggesting that the hydration water of {βCD·PhE} is not only so strongly bound but also corresponds to a smaller amount of water than both in the physical mixture and in βCD. In turn, comparing with the second step of the physical mixture, it is followed by a much more gradual, hence slower, mass loss, ascribed to the guest release subsequent to the dissociation of the inclusion complexes in {βCD·PhE}. The data reinforce the previous conclusions according to which {βCD·PhE} is a true inclusion compound.

Thermograms for {βCD·PhE} and βCD samples, prepared at room temperature and defined RH values (0, 15, 58, 100%), are shown in Fig. 5.

In the βCD thermograms, dehydration occurs in single steps for RHs 0, 15 and 58%, and in two steps, for the fully hydrated sample. The hydration water found in the sample prepared at RH 0% and shown in the corresponding thermogram by the initial step can result from the presence of non-replaceable water molecules in βCD, *i.e.*, of water molecules which do not exchange reversibly with water vapour at room temperature.[1,3] For all the other considered RH values, the dehydration steps end at more or less defined temperatures in the range between 80 and 90 °C, being followed by lines of constant mass, at least, up to the highest recorded temperature (150 °C). A large gap between the percentage mass losses recorded for RHs 58 and 100% suggests that the sample prepared at RH 100% retained a significant amount of free surface water which, in turn, might be responsible for the first observed dehydration step that ends at roughly 55 °C. Hence, the single hydration steps observed at RHs 15 and 58% should correspond, by the temperatures of their respective inflection points, to the second step found for the fully hydrated βCD sample that occurs in the same temperature range, approximately.

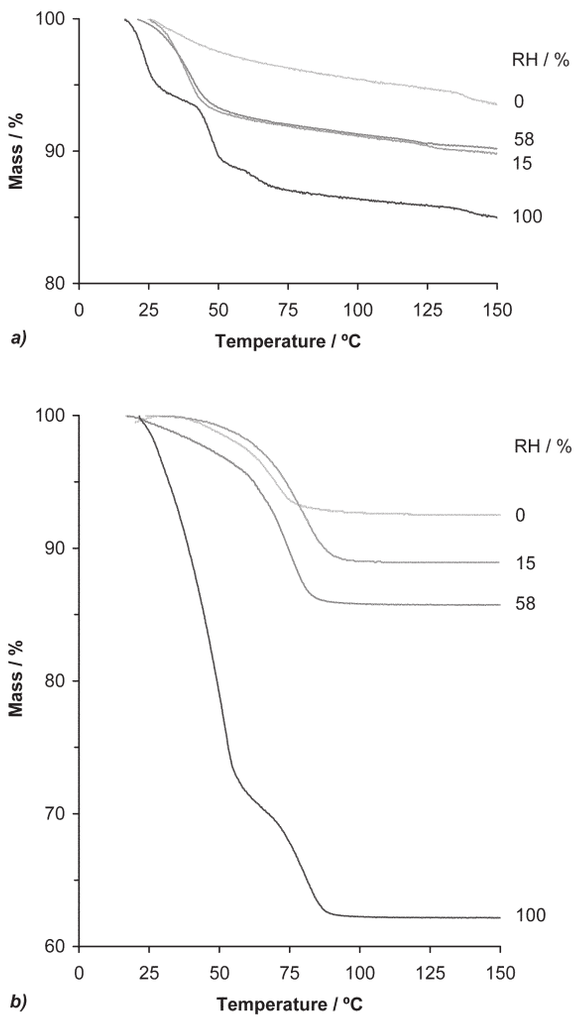

Fig. 5 Thermograms for {βCD·PhE} (a) and βCD (b) samples prepared at defined RHs (0, 15, 58, 100%).

Unlike for βCD, the thermograms for {βCD·PhE} samples prepared at defined RH values do not present zero slope segment lines, in the observed range of temperatures (from room temperature up to 150 °C). In addition, the highest percentage mass losses for the {βCD·PhE} and βCD samples, observed at RH 100%, correspond approximately to 13 and 37%, respectively. Thermograms for RHs 15 and 58% are represented by closely spaced lines which, incidentally, intercept each other at *ca.* 40 °C. In turn, the thermogram for RH 100% shows three dehydration steps up to 71 °C. On the whole, these observations confirm what was already found for {βCD·PhE} and βCD samples at ambient humidity (by its PXRD pattern, the humidity of this sample should correspond to RH slightly over 58%), that is, {βCD·PhE} samples retain less hydration water that is not as strongly bound as in the corresponding samples of βCD at the same RHs. Besides pointing to distinct structures for {βCD·PhE} and βCD, these observations suggest that, in comparison with βCD, {βCD·PhE} allows for a much easier water release and originates a faster water exchange with the environment.

Raman spectra

While no significant differences in Raman shifts were observed upon comparison of the FT-Raman spectrum of {βCD·PhE} with that of the 1:1 physical mixture, relevant variations were registered in the relative intensities of various Raman bands. This should not surprise us, since vibrational Raman spectroscopy is known to be sensitive to weak non-covalent interactions, those that intervene in {βCD·PhE}.

Fig. 6 shows the FT-Raman spectra for {βCD·PhE} and the 1:1 physical mixture, in the 1700–500 cm^{-1} region. Among the bands highlighted, some are affected either by guest encapsulation, as assessed by comparing the spectrum of {βCD·PhE} with that of the 1:1 physical mixture (Fig. 6), or by humidity, as assessed below by comparing spectra at defined RHs (Fig. 7(a) and (b)). They can be generally assigned to various CO stretchings in βCD (band maxima at 1140, 1116, 1088, 1056, 950, 938 and 926 cm^{-1}) and to CH_2 bendings in βCD (band maxima at 865 and 856 cm^{-1}). Since the 950, 938 and 926 cm^{-1} Raman bands are ascribed to the CO stretching vibrations of the α-1,4 linkages, it is expected that these bands will be affected by the relative orientations of the glucose units in the βCD macrocycle, thus sensing the presence of the guest molecule in the βCD cavity. Incidentally, it should be mentioned that a previous Raman optical activity study of βCD has found that a Raman band at around 920 cm^{-1} is sensitive to the conformations around the glycosidic linkage in the βCD macrocycle.[19] Also, the relative intensities of the bands at 865 and 856 cm^{-1}, assigned to CH_2 bendings in βCD with *trans*-C1O5–C5C6 dihedral axes, can be sensitive to guest encapsulation, considering they are adjacent to the disordered primary OH groups.[20]

In the spectrum of the 1:1 physical mixture, a pair of almost equally intense bands occurring at 865 and 854 cm^{-1} originates a prominent band at 865 cm^{-1} and a shoulder in the lower Raman shift wing of this band, in the Raman spectrum of {βCD·PhE} (see inset in Fig. 6). In addition, two Raman

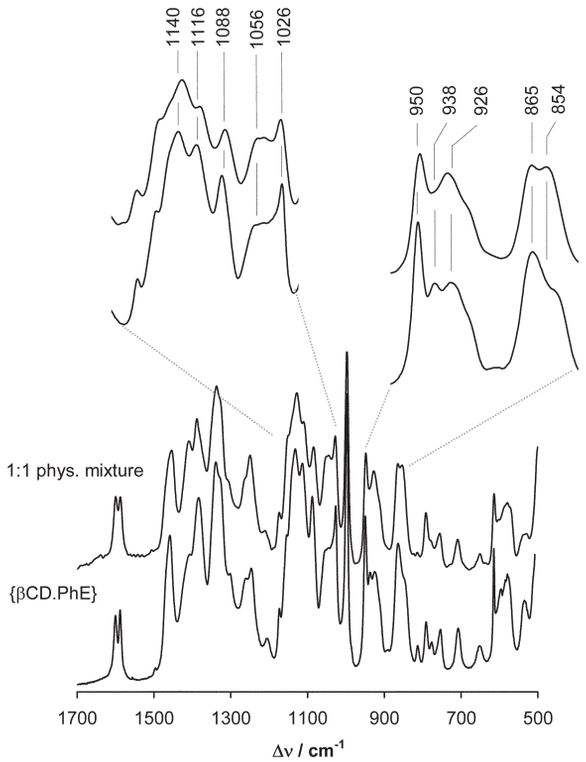

Fig. 6 FT-Raman spectra, between 1700 and 500 cm^{-1}, for samples of {βCD·PhE} and the 1:1 physical mixture of βCD and PhE at ambient humidity.

bands at 950 and 927 cm^{-1} in the spectrum of the 1:1 physical mixture give rise to a pattern of three bands at 950, 938 and 926 cm^{-1} in the Raman spectrum of {βCD·PhE}, with the first band having the higher intensity and the latter two Raman features displaying approximately equal intensities (see inset of Fig. 6).

Considering now the effect of varying RH, Fig. 7 presents the Raman spectra of {βCD·PhE} (a) and βCD (b), at defined RH values (0, 15, 58, 100%), in the 1200–800 cm^{-1} region. In the Raman spectra of {βCD·PhE} (Fig. 7(a)), the 865 cm^{-1} band retains its higher relative intensity at all recorded RH values, in the pair of bands at 865 and 854 cm^{-1}. In addition, in the set of three bands, closely located at 950, 938 and 926 cm^{-1}, the band at 950 cm^{-1} is still the more intense band at all the considered RHs, but the Raman feature at 926 cm^{-1} increases with RH, originating a relatively prominent feature at 924 cm^{-1} when RH attains 100%. Increase in RH leads also to a relatively minor increase in the intensity for the 1056 cm^{-1} Raman feature in relation to the almost RH-independent Raman band at 1026 cm^{-1}, especially visible for RH 100%. The latter band is ascribed to a predominantly PhE Raman band, since it does not show up in the spectra of βCD at any defined RH. In these spectra, a shoulder appears in the lower Raman shift wing of a band at 1047 cm^{-1}.

The bands whose maxima occur at 1056 cm^{-1} and 924 cm^{-1} in the spectrum of {βCD·PhE} at RH 100% are tentatively assigned to νC6O6 and to νCO involving the α-1,4 linkages, respectively. Hence, their intensity sensitivity to RH variation comes as no surprise. On one hand, the C6O6 bonds are adjacent to the disordered primary OH groups which, in turn, can be involved in hydrogen bonding interactions. On the other hand, the CO α-1,4 bonds are expected to be sensitive to the orientations of the glucose units in the βCD macrocycle, thus sensing the presence and orientation of the guest molecule inside the βCD cavity which, in turn, can both be affected by RH.

Since water molecules inside the βCD cavity are not hydrogen bonded to the βCD atoms but tend to cluster instead, thus

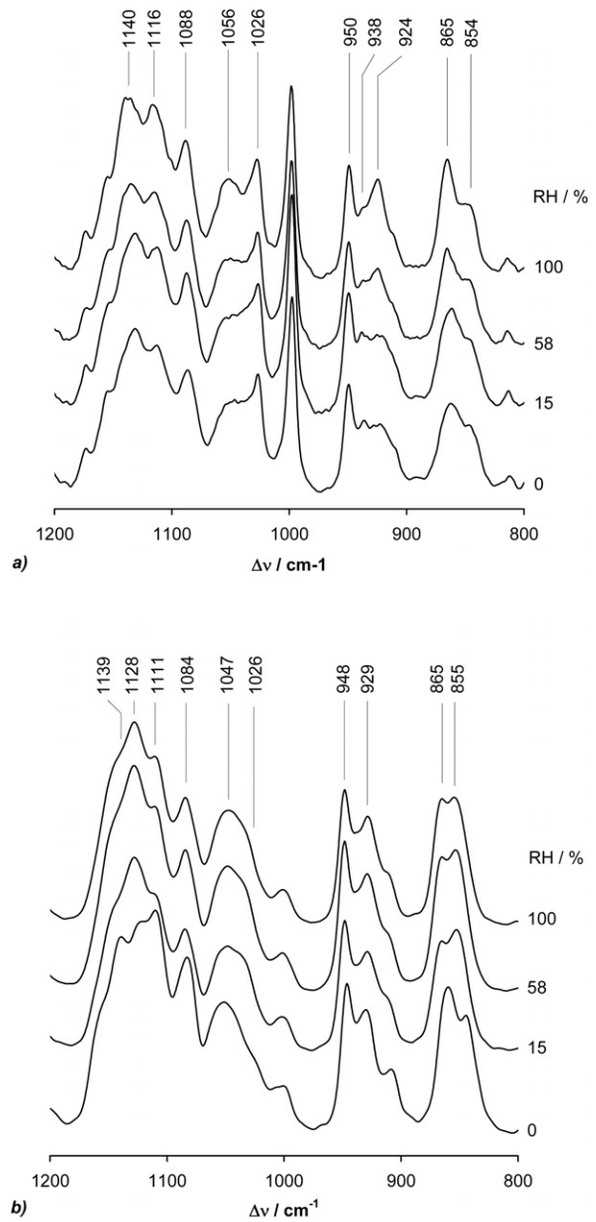

Fig. 7 FT-Raman spectra in the 1200–800 cm^{-1} region for samples of {βCD·PhE} (a) and βCD (b) at defined RHs (0, 15, 58, 100%).

interacting with the βCD atoms by van der Waals interactions, it may be difficult to distinguish, by Raman spectroscopy, their presence in the βCD cavity from that of a guest molecule. In fact, as a general comment to the Raman spectra of βCD at defined RH values (Fig. 7(b)), one should mention that no relevant intensity variations are observed when RH is equal or higher than 15%. However, the Raman spectrum of βCD at RH 0% exhibits important relative intensity variations both in the pair of bands at 865 and 855 cm^{-1} and in the set of three Raman bands at 1139, 1128 and 1111 cm^{-1} (frequency values given for RH 100%).

^{13}C CP MAS NMR

The solid-state ^{13}C CP MAS NMR spectrum for {βCD·PhE} is presented in Fig. 8, together with the spectrum of βCD, for comparison. The latter shows multiple resonances for each type of carbon atom (C1, C4, C2,3,5, C6). These have been mainly correlated with as many slightly different orientations of the glucose units in the βCD macrocycle, *i.e.*, with distinct

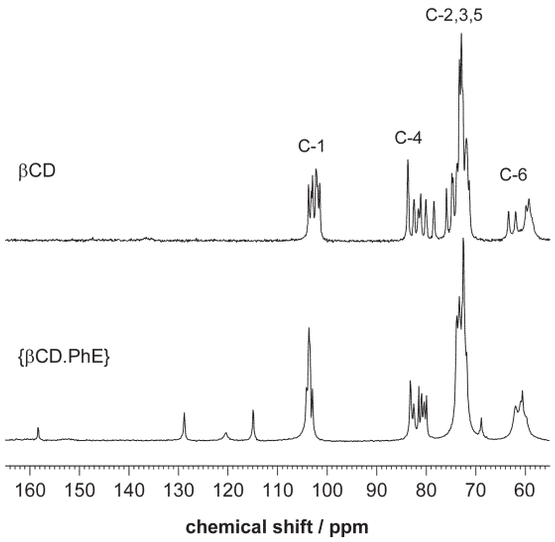

Fig. 8 ^{13}C CP MAS NMR spectra for samples of βCD and {βCD·PhE} at ambient humidity.

torsion angles about the (1→4) linkages for C1 and C4, and with distinct orientations of the primary hydroxyl groups, for C6.[9,12] While the centres of the multiple resonances observed for each type of carbon atom in the {βCD·PhE} and βCD spectra roughly coincide, the multiplicity of resonances and the dispersion of observed chemical shifts (*i.e.*, the chemical shift range that comprises all the resonances from the same carbon atom in distinct glycosidic units) decrease appreciably in passing from βCD to {βCD·PhE} (see values in Table 1). This finding suggests a greater equivalence of the various carbon atoms of each type in {βCD·PhE} with respect to βCD, presumably due to the improved symmetrization of the βCD macrocycle in the channel structure of {βCD·PhE}.[9,11,21]

The ^{13}C CP MAS NMR spectra for {βCD·PhE} and βCD, at defined RHs (0, 15, 20, 58, 100%), are presented in Figs. 9 and 10, respectively, in the chemical shifts range for the cyclodextrin carbon atoms. Starting with the spectra for {βCD·PhE} at defined RH values (Fig. 9), the first general observation is that these spectra are affected by the hydration level. Among the considered RH values, spectra for RHs 0 and 15% are clearly distinct from the spectra for the remaining RHs, since they present wide and uncharacteristic features very much in consonance with an amorphous solid for these RH values due to the loss of water. In turn, for RHs 20, 58 and 80% (not shown), no discernible trend, either on the multiplicity of resonances or on the dispersion of chemical shifts values, is observed by varying RH. In turn, in the fully hydrated {βCD·PhE} (RH 100%), apart from changes in the C1 and C4 overall signal shapes, a small chemical shift of C6 towards lower chemical shifts, *i.e.*, to higher field, is worth mentioning.

Considering now the ^{13}C CP MAS NMR spectra for crystalline βCD at various defined RHs, the spectrum at RH 0% for the collapsed crystalline structure is distinct from the spectra for the remaining RHs. But, unlike the corresponding

Table 1 Dispersion of chemical shifts values (ppm) for βCD carbon atoms in {βCD·PhE} and in crystalline βCD

	Chemical shift/ppm			
System	C-1	C-4	C-2,3,5	C-6
βCD	4.4	6.9	6.2	7.2
{βCD·PhE}	3.2	4.9	5.9	4.0

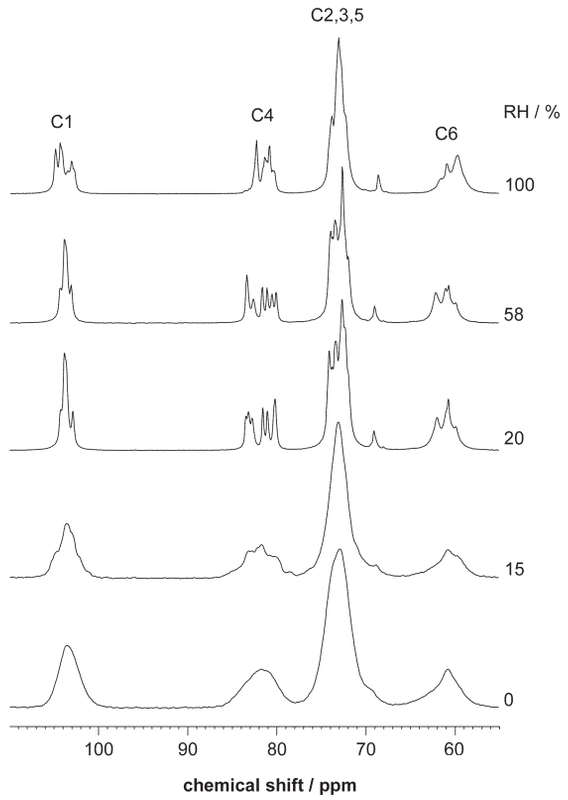

Fig. 9 ^{13}C CP MAS NMR spectra for samples of {βCD·PhE} at defined RHs (0, 15, 20, 58, 100%) in the βCD carbon atoms chemical shifts range.

spectrum for {βCD·PhE}, the βCD spectrum at RH 0% presents sharp multiple resonances for each type of carbon atom.[22] Between RHs 15 and 100%, the spectra stay almost unchanged in the general parameters so far considered,

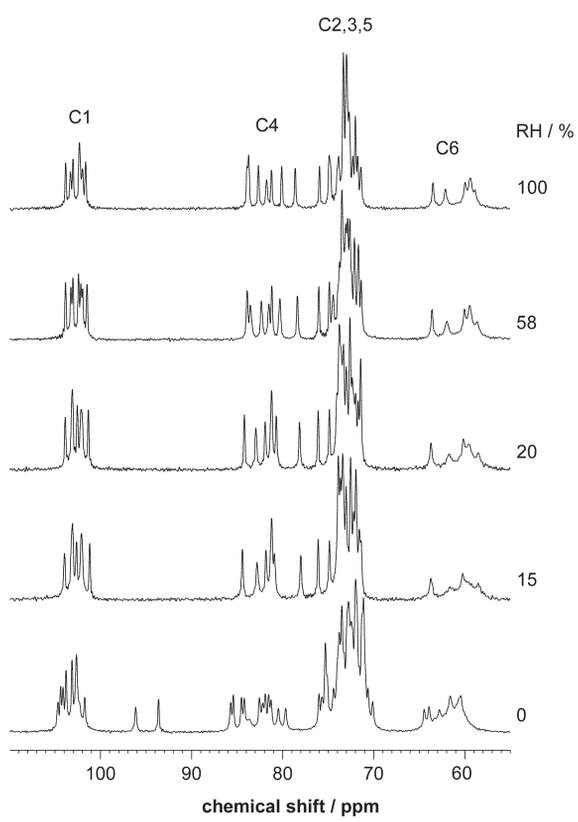

Fig. 10 ^{13}C CP MAS NMR spectra for samples of βCD at defined RHs (0, 15, 20, 58, 100%).

namely, chemical shift changes for the centres of the various carbon atoms resonances, their multiplicities, and dispersions of the chemical shifts values.

Comparison of the ^{13}C CP MAS NMR spectra for {βCD·PhE} and βCD at corresponding RH values equal or higher than RH 20% reveals, as a general trend, a reduced multiplicity and a diminished dispersion of chemical shifts values for each type of carbon atom in {βCD·PhE} with respect to βCD.

Acknowledgements

We are grateful to Fundação para a Ciência e Tecnologia, Lisboa, for partial founding (SFRH/BD/1101/2000). We also thank Ms Paula Esculcas for assistance in the NMR experiments and Ms Rosário Soares for assistance in the PXRD experiments.

References

1 T. Steiner and G. J. Koellner, *J. Am. Chem. Soc.*, 1994, **116**, 5122.
2 T. Steiner, A. M. Moreira da Silva, J. J. C. Teixeira-Dias, J. Müller and W. Saenger, *Angew. Chem., Int. Ed.*, 1995, **34**, 1452.
3 A. Marini, V. Berbenni, G. Bruni, V. Massarotti, P. Mustarelli and M. Villa, *J. Chem. Phys.*, 1995, **103**, 7532.
4 A. M. Moreira da Silva, T. Steiner, W. Saenger, J. A. Empis and J. J. C. Teixeira-Dias, *Chem. Commun.*, 1996, 1871.
5 J. E. H. Koehler, W. Saenger and W. F. Gunsteren, *Eur. Biophys. J.*, 1987, **15**, 211.
6 R. G. Winkler, S. Fioravanti, G. Ciccotti, C. Margheritis and M. Villa, *J. Comput.-Aided Mol. Des.*, 2002, **14**, 659.
7 K. Braesicke, T. Steiner, W. Saenger and E. W. Knapp, *J. Mol. Graph. Modell.*, 2000, **18**, 143.
8 M. G. Usha and R. J. Wittebort, *J. Am. Chem. Soc.*, 1992, **114**, 1541–1554.
9 M. J. Gidley and S. M. Bociek, *J. Am. Chem. Soc.*, 1988, **110**, 3820.
10 S. J. Kitchin and T. K. Halstead, *Solid State Nucl. Magn. Reson.*, 1996, **7**, 27.
11 S. F. Tanner, S. G. Ring, M. A. Whittam and P. S. Belton, *Int. J. Biol. Macromol.*, 1987, **9**, 219.
12 S. J. Heyes, N. J. Clayden and C. M. Dobson, *Carbohydr. Res.*, 1992, **233**, 1.
13 P. Job, *Ann. Chim. (Paris)*, 1928, **9**, 113.
14 L. Cunha-Silva and J. J. C. Teixeira-Dias, *J. Inclusion Phenom. Macrocycl. Chem.*, 2002, **43**, 127.
15 Z. Metzafos, I. M. Mavridis and M. B. Hursthouse, *Acta Crystallogr., Sect. C*, 1996, **52**, 1220.
16 PowderCell, version 2.4, W. Kraus and G. Nolze, Federal Institute for Materials Research and Testing, Rudower Chaussee 5, 12489 Berlin, Germany.
17 M. R. Caira, *Rev. Roum. Chim.*, 2001, **46**, 371.
18 Z. Metzafos, I. M. Mavridis, G. Le Bas and G. Tsoucaris, *Acta Crystallogr., Sect. B*, 1991, **47**, 746.
19 A. F. Bell, L. Hecht and L. D. Barron, *Chem. Eur. J.*, 1997, **3**, 1292.
20 T. Steiner, W. Saenger and R. E. Lechner, *Mol. Phys.*, 1991, **72**, 1211.
21 L. Cunha-Silva and J. J. C. Teixeira-Dias, *J. Phys. Chem.*, 2002, **106**, 3323.
22 Two peaks (at approximately 96 and 94 ppm) occur at RH 0% in an unusual part of the spectrum for cyclodextrins. The assignment of these two peaks is not clear. In fact, considerations of intensities seem to indicate that they are C4, whereas chemical shift considerations suggest that they are C1 peaks.[11].